

Single-shot detection and direct control of carrier phase drift of midinfrared pulses

Cristian Manzoni,* Michael Först, Henri Ehrke, and Andrea Cavalleri

Max Planck Research Group for Structural Dynamics, University of Hamburg, Center for Free Electron Laser Science, c/o DESY, Notkestraße, 85–22607 Hamburg, Germany

*Corresponding author: cristian.manzoni@mpsd.cfel.de

Received December 14, 2009; revised January 25, 2010; accepted January 26, 2010; posted January 29, 2010 (Doc. ID 121498); published February 26, 2010

We introduce a scheme for single-shot detection and correction of the carrier-envelope phase (CEP) drift of femtosecond pulses at mid-IR wavelengths. Difference frequency mixing between the mid-IR field and a near-IR gate pulse generates a near-IR frequency-shifted pulse, which is then spectrally interfered with a replica of the gate pulse. The spectral interference pattern contains shot-to-shot information of the CEP of the mid-IR field, and it can be used for simultaneous correction of its slow drifts. We apply this technique to detect and compensate long-term phase drifts at 17 μm wavelength, reducing fluctuations to only 110 mrad over hours of operation. © 2010 Optical Society of America
OCIS codes: 230.4320, 320.5550.

Intense pulses at terahertz (THz) frequencies allow for the control of various dynamic processes in condensed matter. Among these processes, vibrationally driven phase transitions in highly correlated electron systems [1,2] provide an interesting new direction of research, which could be extended to a number of excitations in condensed phases. Especially important is the ability to control these excitations directly with THz or mid-IR (MIR) electric fields well defined in frequency and phase. The evolution of such processes can be followed by time-resolved techniques, which require synchronization of ultrashort probe pulses with the exciting electric field.

One parameter for the description of the electric field of few-cycle pulses is the carrier envelope phase (CEP), which defines the temporal offset of the peak of the intensity envelope from the nearest peak of the carrier wave. The generation of pulses with reproducible electric field thus calls for the control of the CEP (see, e.g., [3] for a review). Nonlinear optical processes provide useful tools for the manipulation of CEP and the generation of CEP-stable pulses. Unsaturated difference frequency (DF) mixing between pulses at different frequencies with carrier-envelope phases ϕ_1 and ϕ_2 , generates a pulse with absolute phase given by [4]:

$$\phi_{\text{DF}} = \phi_1 - \phi_2 - \pi/2. \quad (1)$$

When the two waves are derived from the same laser source or are different components of a broadband pulse, they are mutually phase locked, and their phases can be written as $\phi_1 = \phi_2 + \Delta\phi$, where $\Delta\phi$ is their constant phase difference; the difference frequency process then generates a wave with phase $\Delta\phi - \pi/2$. Following this idea, phase-stable near-IR and MIR pulses have been generated by mixing two spectral portions of a single broadband pulse [5,6]; THz generation by optical rectification, which produces long wavelength radiation with a stable CEP from an unstable near-IR pulse, can also be understood in these terms [7]. Other schemes are based on difference-frequency generation (DFG) between two

synchronized pulses of different carrier frequencies [8]; in this case, high stability of the path lengths of the two interacting pulses is required, since any temperature or mechanical fluctuation and long-term drift directly influences the CEP of the generated beam. The ability to detect and instantaneously correct spurious CEP drifts becomes therefore crucial when performing phase-sensitive measurements. In the visible and the near-IR, f -to- $2f$ interferometry [9] can reliably detect real-time CEP jitter [10,11]. For THz pulses, many sophisticated techniques for single-shot detection of the electric field have been proposed, based on electro-optic (EO) sampling combined with noncollinear geometries [12], echelon optics [13], or pulse-front tilting [14].

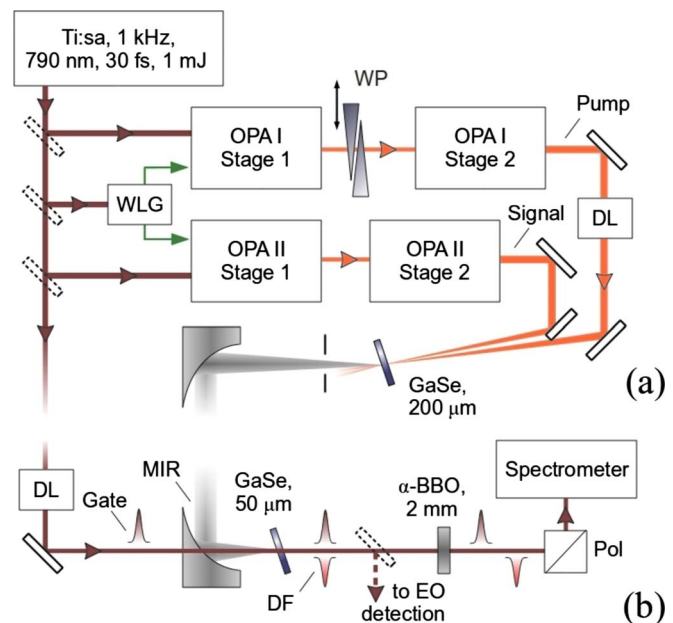


Fig. 1. (Color online) (a) Setup for the production of tunable light pulses at mid-infrared wavelengths. (b) Scheme for the detection of MIR CEP drift. WLG, white-light generation; DL, delay lines; WP, wedge plates; DF, difference frequency pulse; EO, electro-optic.

In this Letter, we introduce a simple scheme for single-shot monitoring and slow correction of absolute-phase drifts in the MIR spectral range. The detection technique is based on the DF mixing between the MIR field (with phase ϕ_{MIR}) and a gate pulse (with phase ϕ_{Gate}), and on spectral interferometry between the gate and the DF field. According to Eq. (1), the DF pulses have absolute phase of $\phi_{\text{Gate}} - \phi_{\text{MIR}} - \pi/2$: spectral interference between the gate and the DF pulse thus gives rise to a fringe pattern, which, in the frequency domain, has phase $\phi_{\text{Gate}} - (\phi_{\text{Gate}} - \phi_{\text{MIR}} - \pi/2) + \text{const} = \phi_{\text{MIR}} + \text{const}$. The interference therefore allows single-shot retrieval [15] of the absolute-phase jitter of the MIR pulse, and it is independent from the carrier-envelope phase of the gate pulse. We apply this technique to measure short- and long-time phase stability of our pulses at 17 μm carrier wavelength, and we use it to simultaneously compensate for long-term phase drifts, stabilizing the absolute phase over hours of operation.

The experimental setup for the generation of tunable MIR pulses is given in Fig. 1(a): it is based on two noncollinear two-stage IR optical parametric amplifiers (OPAs) [8] powered by an amplified Ti:sapphire laser, providing 30 fs, 1 mJ pulses at 790 nm wavelength and 1 kHz repetition rate. OPA I delivers pulses tuned to 1.3 μm wavelength with energy of 160 μJ , and OPA II generates 130 μJ pulses at 1.41 μm ; the pulses are labeled pump and signal, respectively. To phase lock them, both OPAs are seeded by the same white light, obtained by self-phase modulation in a 2-mm-thick sapphire plate. The beams from the two OPAs are then combined in a 200 μm thick z -cut GaSe, oriented for Type II DFG; the process provides 2.5 μJ phase-stable MIR pulses at a wavelength of about 17 μm (≈ 17.6 THz frequency).

The setup for phase-drifts detection is depicted in Fig. 1(b): the MIR pulses are combined with a fraction of the laser source pulses, acting as gate, in a 50 μm thick z -cut GaSe crystal for DFG. A hole drilled in the gold off-axis parabolic mirror allowed collinear combination of the two beams. Their polarizations and the orientation of the crystal were adjusted for Type II [$e(\text{MIR}) + o(\text{DF}) \rightarrow e(\text{Gate})$] interaction. The copropagating, cross-polarized gate and DF pulses were then relatively delayed to about 1 ps by a 2-mm-thick α -barium borate plate, projected to the same polarization by an achromatic polarizer and directed to a spectrometer. The described nonlinear process was also feasible for EO sampling [16,17] of the MIR electric field (see dashed line in Fig. 1). In Fig. 2 we report the spectra of gate (dashed-dotted line) and DF pulses (solid line), together with the fringes arising from their balanced interaction (inset). High-contrast interference pattern could be detected with MIR peak intensities as low as 1 GW/cm^2 . Note that since the gate pulse is locally shorter than one MIR optical cycle; in the frequency domain this corresponds to having the gate bandwidth broader than the MIR carrier frequency, which

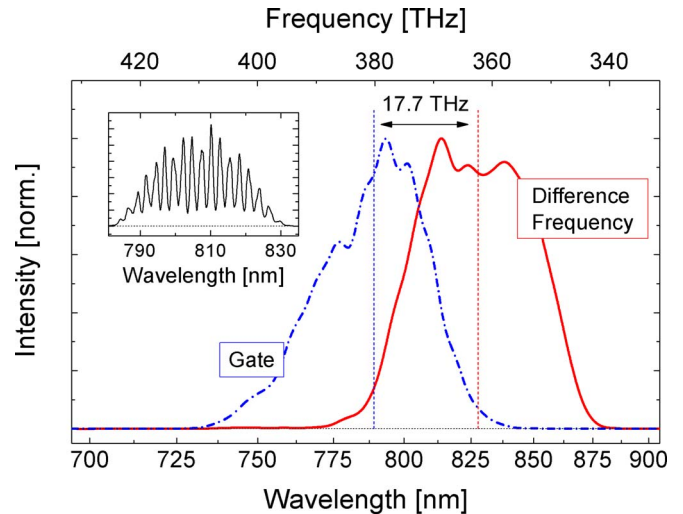


Fig. 2. (Color online) Spectra of the gate (blue dashed-dotted line) together with the side band (red solid line) arising from difference frequency mixing with the MIR pulses in a GaSe crystal. The weighted center of each spectrum is also given. Inset, fringe pattern from balanced spectral interference between gate and DF pulses.

automatically leads to spectral overlap with the DF light. This is the same requirement of EO-sampling techniques, basically relying on similar processes [17].

Figure 3 shows the effect of a phase shift artificially induced on the MIR pulse, measured by the corresponding fringe pattern and with EO sampling. The MIR phase was adjusted by acting on the phase difference $\Delta\phi$ between the two OPAs before the MIR generation, i.e., by changing the pump beam path with a fused-silica wedge pair, placed before the saturated second stage of OPA I and equipped with a high-resolution stepper motor. Panels (a) and (b) show a sequence of fringe patterns and the retrieved phase shift after the introduction of 3.5 μm of glass in the pump beam path: the traces exhibit a clear shift of 7.2 rad, which is in very good agreement with

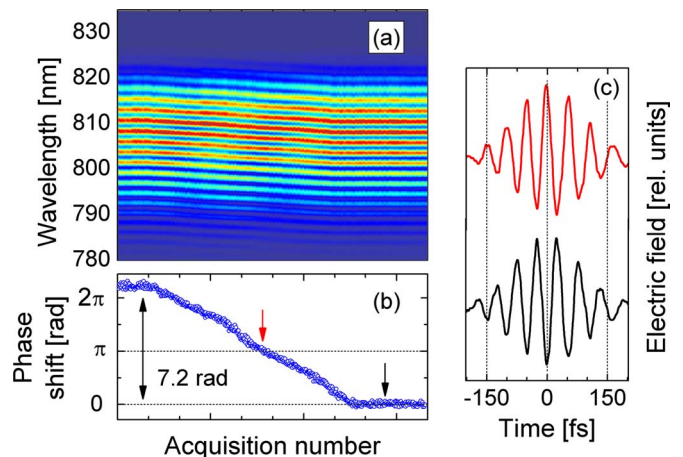


Fig. 3. (Color online) (a) Sequence of spectra acquired during the introduction of 3.5 μm of fused silica glass on the pump beam path and (b) corresponding phase shift. (c) Electric field deduced from EO sampling of the MIR pulses for the two phase values indicated by the arrows in panel (b).

the calculated increase of $\Delta\phi$ by 7.6 rad. In panel (c) we also report the pulse electric field measured by EO sampling at the detected phase values indicated by the arrows, corresponding to a shift of π rad. The phase shift of the interference pattern and its good agreement with both the expected value and the EO-sampling traces are clear proofs that our scheme can detect phase drifts of MIR pulses. The system was then applied to the characterization of the CEP of our MIR source. Although the technique can in principle follow carrier phase drifts on a single-shot basis, we could acquire spectra only every 8 ms owing to the limited readout rate of our spectrometer; sequences of fringe patterns acquired for 15 s showed a phase jitter with an rms of 80 mrad, demonstrating excellent short-term CEP-stability of the MIR pulses. However, significant drift was observed when monitoring the MIR pulses for hours of free-running operation. Figure 4 shows that the CEP accumulates a drift of more than π rad over 1 h. This slow drift could be directly compensated by acting on the wedge pair in the beam pump. To this end, we applied a low-pass filter with time constant of 6 s to the instantaneous phase jitter to provide the feedback signal. The position of the wedges was proportionally updated every 1 s. This control system was tested for more than 2 h and displayed excellent capabilities to follow and correct low-frequency phase drifts. The black data in Fig. 4 show the retrieved MIR absolute phase when the control system was active; the recorded trace shows fluctuations with rms $\sigma=110$ mrad.

The reported values can be compared to errors introduced by the detection scheme owing to: (i) instabilities in the DF-gate pathlength and in the retrieval algorithm, which together introduced a jitter with rms of 25 mrad; (ii) slow fluctuations of the gate-MIR delay, which shifts the position of the scanning gate with respect to the MIR carrier: in this case

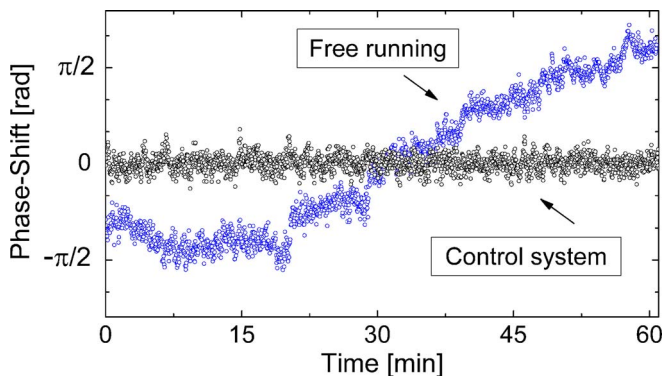


Fig. 4. (Color online) Long-term characterization of the MIR phase drift. Both free-running and closed loop measurements are displayed.

we estimated a drift of the order of 1 fs, corresponding to an error of 110 mrad in the measurement of the 17 μm carrier phase. Other errors may be introduced if the DF process is driven at saturation. For this reason care was taken in order to operate in the linear regime.

In conclusion, we have introduced a scheme for single-shot characterization of the short- and long-term absolute-phase drifts of MIR pulses. Measurements on self-phase stabilized MIR light generated via a DF process conveyed that these pulses exhibit a phase jitter with $\sigma=80$ mrad over 15 s, and a drift of π rad over 1 h. A control loop enables the compensation of this slow drift to 110 mrad only. The very low peak intensity of the MIR pulses required to detect the fringe patterns allows for easy implementation of this technique in parallel with time-resolved spectroscopic measurements.

References

1. M. Rini, R. Tobey, N. Dean, J. Itatani, Y. Tomioka, Y. Tokura, R. W. Schoenlein, and A. Cavalleri, *Nature* **449**, 72 (2007).
2. R. I. Tobey, R. Prabakharan, A. T. J. Boothroyd, and A. Cavalleri, *Phys. Rev. Lett.* **101**, 197404 (2008).
3. T. Brabec and F. Krausz, *Rev. Mod. Phys.* **72**, 545 (2000).
4. A. Baltuška, T. Fuji, and T. Kobayashi, *Phys. Rev. Lett.* **88**, 133901 (2002).
5. C. Vozzi, C. Manzoni, F. Calegari, E. Benedetti, G. Sansone, G. Cerullo, M. Nisoli, S. De Silvestri, and S. Stagira, *J. Opt. Soc. Am. B* **25**, B112 (2008).
6. X. Huber, A. Brodschelm, F. Tauser, and A. Leitenstorfer, *Appl. Phys. Lett.* **76**, 3191 (2000).
7. J. Hebling, K.-L. Yeh, M. C. Hoffmann, B. Bartal, and K. A. Nelson, *J. Opt. Soc. Am. B* **25**, B6 (2008).
8. A. Sell, A. Leitenstorfer, and R. Huber, *Opt. Lett.* **33**, 2767 (2008).
9. M. Kakehata, H. Takada, Y. Kobayashi, K. Torizuka, Y. Fujihira, T. Homma, and H. Takahashi, *Opt. Lett.* **26**, 1436 (2001).
10. R. Zinkstok, S. Witte, W. Hogervorst, and K. Eikema, *Opt. Lett.* **30**, 78 (2005).
11. G. Cirmi, C. Manzoni, D. Brida, S. De Silvestri, and G. Cerullo, *J. Opt. Soc. Am. B* **25**, B62 (2008).
12. J. Shan, A. S. Weling, E. Knoesel, L. Bartels, M. Bonn, A. Nahata, G. A. Reider, A. Georg, and T. Heinz, *Opt. Lett.* **25**, 426 (2000).
13. K. Y. Kim, B. Yellampalle, A. J. Taylor, G. Rodriguez, and J. H. Glowina, *Opt. Lett.* **32**, 1968 (2007).
14. Y. Kawada, T. Yasuda, H. Takahashi, and S.-I. Aoshima, *Opt. Lett.* **33**, 180 (2008).
15. L. Lepetit, G. Chériaux, and M. Joffre, *J. Opt. Soc. Am. B* **12**, 2467 (1995).
16. K. Liu, J. Xu, and X. C. Zhang, *Appl. Phys. Lett.* **85**, 863 (2004).
17. C. Kübler, R. Huber, S. Tübel, and A. Leitenstorfer, *Appl. Phys. Lett.* **85**, 3360 (2004).